Molecular Determinants of Steroid Inhibition for the Mouse Constitutive Androstane Receptor

Johanna Jyrkkärinne,[†] Janne Mäkinen,[†] Jukka Gynther,[§] Heidi Savolainen,[†] Antti Poso,[§] and Paavo Honkakoski*,[†]

Departments of Pharmaceutics and Pharmaceutical Chemistry, University of Kuopio, P.O.Box 1627, FIN-70211 Kuopio, Finland

Received April 3, 2003

The constitutive androstane receptor (CAR) regulates drug and steroid metabolism through binding to cytochrome P450 *2B*, *2C*, and *3A* gene enhancers. Uniquely among nuclear receptors, mouse CAR (mCAR) can be suppressed by androstenol and activated by structurally diverse drugs, pesticides, and environmental pollutants. To gain insight into presently ill-defined structural requirements of mCAR ligands, we employed a mCAR inhibition assay in mammalian HEK293 cells to create a QSAR model that could well predict the inhibition by three unknown steroids. Two novel mCAR inhibitors were thus identified. Yeast two-hybrid assays indicated that steroids inhibit mCAR primarily by promoting association of mCAR with the corepressor NCoR, with only minor contribution from other mechanisms. Analysis of chimeric and mutant mCAR constructs suggested that androstenol sensitivity is controlled by residues between amino acids 201−263 (helices 5−7) and it does not depend on the residue 350 within helix 12, as previously suggested.

Introduction

Nuclear receptors (NRs) are ligand-dependent transcription factors that control cellular development and homeostasis,[1,2] and they are important targets for medicinal chemistry. Humans have 48 NR genes which can be classified based on sequence similarities within domains required for DNA-binding (DBD) and ligand-binding (LBD).[3] Agonist binding induces conformational changes in the LBD (especially movement of the C-terminal helix 12) that leads to formation of a hydrophobic surface to which NR coactivators can bind.[4,5] NR coactivators such as SRC-1 transmit the signal to gene promoters in a process involving histone acetylation, loosening of chromatin structure, and activation of gene transcription.[6] In contrast, antagonist binding will prevent reorientation of helix 12 and promote association between the LBD and NR corepressors such as NCoR. This interaction ultimately leads to histone deacetylation and gene repression.[7] Finally, partial agonists have transcriptional activity despite their apparent inability to reorient helix 12 to agonistic conformation.[5,8]

The mouse constitutive androstane receptor (mCAR; NR1I3) controls the drug inducibility of cytochrome P450 2B (*CYP2B*) genes through its binding to the *p*heno*b*arbital-*r*esponsive DNA *e*nhancer *m*odule PBREM.[9−12] Other mCAR target genes include drug and steroid metabolizing enzymes, transport proteins, and enzymes associated with glucose and lipid metabolism.[11−13] Intriguingly, in the absence of any added ligand, mCAR has considerable basal activity which can be suppressed by 5α-androst-16-en-3α-ol (androstenol), i.e., androstenol acts as an inverse agonist.[14,15] Many *CYP2B* inducers such as 1,4-bis[2-(3,5-dichloropyridyloxy)]benzene (TCPOBOP), chlorpromazine, metyrapone, clotrimazole, and methoxychlor are able to reactivate the androstenol-suppressed mCAR, and some compounds even 'super-activate' mCAR to levels above the basal activity.[16−19]

However, the structural requirements of mCAR ligands and their mechanisms of action are not clear for several reasons. At present, mCAR has not been crystallized; *CYP2B* inducers and mCAR activators do not show any quantitative structure−activity relationship (QSAR) or even share clear structural features; and finally, the data on the inhibition of mCAR by steroids are limited and even contradictory. For instance, it was reported that the full-length mCAR was activated by estradiol but efficiently inhibited by testosterone and progesterone in HepG2 cells.[20] Others have not seen such inhibition by testosterone in CV-1 or HEK293 cells.[15,19] Androstenol was found to dissociate the coactivator SRC-1 from the mCAR LBD in vitro,[15] although in later studies the degree of dissociation appears variable and modest.[17,21]

Consequently, no valid three-dimensional QSAR (3D-QSAR) analysis has been published for mCAR inhibitors or activators. Apart from TCPOBOP and androstenol, other modulators of mCAR activity have been reported, although formal demonstration that they mediate their effects via the mCAR LBD is often missing. This would be necessary for the construction of a QSAR model because such models generally assume a single effector site for biological activity. Because the full-length mCAR activity could, in principle, be affected at the level of DNA binding or heterodimerization with retinoid X receptor (RXR), it would be useful to devise an assay that would minimize these effects. Therefore, we used an assay that is based on the GAL4-mCAR LBD fusion

* Correspondence to Paavo Honkakoski. Telephone: +358-17-162490. Fax: +358-17-162252. E-mail: paavo.honkakoski@uku.fi.
[†] Department of Pharmaceutics.
[§] Department of Pharmaceutical Chemistry.

10.1021/jm030861t CCC: $25.00
Published on Web 09/27/2003

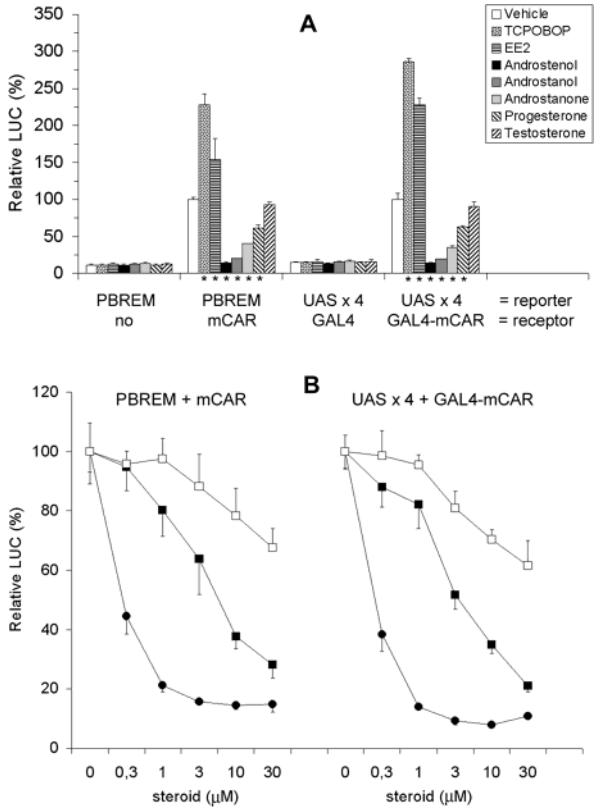

Figure 1. Inhibition of mCAR activity in mammalian HEK293 cells. A. Responses of the full-length mCAR-driven PBREM-tk-luc and GAL4-mCAR-driven UASx4-tk-luc reporters to vehicle, 1 μM TCPOBOP, and indicated 10 μM steroids. The data point with receptor and vehicle was set to 100% for both reporters. An asterisk below a column indicates a statistically significant difference ($p < 0.05$) from the vehicle control. B. Dose−responses of PBREM-tk-luc and UASx4-tk-luc reporter activity by androstenol (●), androstanone (■), and testosterone (□) at indicated concentrations. Vehicle control activity was set at 100%. The data are means ± SD of three independent experiments.

protein and assayed over 40 steroids to define the molecular determinants of steroid inhibition of mCAR. Using this biological data set, we generated a model for mCAR inhibitors that was used to predict novel inhibitors. The mechanisms of mCAR inhibition were explored by yeast two-hybrid interactions assays with corepressor NCoR and coactivator SRC-1. Finally, the regions important for androstenol sensitivity were located through the use of chimeric and mutant CAR proteins.

Results

Mammalian mCAR Inhibition Assay. Known mCAR activators TCPOBOP and 17α-ethynyl-3,17β-estradiol (EE2),[17,22] established inhibitors androstenol, androstanol, and androstanone,[15,17] and reported inhibitors progesterone and testosterone[20] were tested to ensure that the GAL4-mCAR LBD fusion protein faithfully mimics the full-length mCAR (Figure 1A). In the absence of receptor, both PBREM-tk-luc and UAS_4-tk-luc reporters were unresponsive to any of these compounds. When full-length mCAR was present, PBREM-driven reporter activity was activated by TCPOBOP (2.3-fold) and EE2 (1.5-fold) and inhibited in decreasing efficiency by androstenol to testosterone (over a range of 91% to 13%, respectively). The GAL4-mCAR LBD showed a slightly greater activation by TCPOBOP (2.9-fold) and EE2 (2.2-fold) but a very similar pattern of inhibition by steroids as the full-length mCAR. Cotransfection of the heterodimer partner RXRα in these assays did not affect the extent of inhibition or the rank order of inhibitors (data not shown). The IC_{50} values for androstenol, androstanone, and testosterone (about 0.2, 3, and >30 μM, respectively) were also very similar between the full-length mCAR and the GAL4-mCAR LBD systems (Figure 1B). These data indicate that the inhibition of mCAR by steroids was dependent only on the mCAR LBD, and that the inhibitors could be ranked reliably by the GAL4-mCAR LBD assay.

Molecular Modeling. Using the above assay, 43 different steroids were evaluated (Table 1), superimposed (Figure 2A) and contrasted to the structure of androstenol (Figure 2B). Initial processing of the data yielded a PLS model with three PLS components with the following statistics: $q^2 = 0.57$, SDEP = 0.45 and $r^2 = 0.80$ (correlation between experimental and predicted pIC_{50} values). These initial values indicate a good model ($q^2 > 0.5$), and only two compounds (4-androsten-7α-ol-3,17-dione and pregnenolone) turned out to be outliers in the PLS plot (data not shown). When these outliers were omitted from the analysis, the statistics slightly improved: $q^2 = 0.59$, SDEP = 0.42 and $r^2 = 0.83$. In the following step, the SRD method with F-factorial selection was used to remove those molecular field properties which did not correlate with mCAR inhibition. The final model statistics are two PLS components, $q^2 = 0.70$, SDEP = 0.35, and $r^2 = 0.82$. These parameters indicate a simple and quite reliable model.[23] The PLS coefficient map (Figure 2C) shows molecular field properties that are correlated with changes in mCAR inhibition.

As an external check of the model, the prediction of mCAR inhibition by three "test set" molecules was performed (Table 2). These unknown steroids were not included in the construction of the model. Predictions for AOCA and ADIEN fell within 0.2−0.3 log units, and for ADIONE within 0.6 log units of the experimental pIC_{50}. The external SDEP value, with two PLS components, was 0.40. The statistics from GOLPE, especially q^2 and both internal and external SDEP values, are good enough to allow more detailed analysis of 3D-QSAR.[23] According to the GOLPE field (Figure 2C), there are four "allowed" regions (green fields near atoms C3, C5, C16, and C19) and three "disallowed" regions (yellow fields near atoms C3, C15, and C16−17) within the model. The allowed regions indicate areas where repulsion between the water probe and the steroid correlates positively with inhibition potency; these areas are probably not populated by mCAR amino acids and hence are free for inhibitor molecule. Conversely, in the disallowed regions, attraction between the probe and the steroid is correlated with stronger inhibition. This volume is probably populated by mCAR amino acids; if an inhibitor includes atoms overlapping with these disallowed regions it would create steric and/or electrostatic "clash" with the receptor. The allowed regions near atoms C19 and C5 are reflecting the positive effects of the 19-methyl group and the single bond C4−C5, respectively, to mCAR inhibition. That is, the loss of

Table 1. Inhibition of mCAR Activity by 43 Steroids[a]

molecule name	remaining activity at 10 μM (%)	estimated pIC_{50}	molecule name	remaining activity at 10 μM (%)	estimated pIC_{50}
cortisone	80 ± 2	4.40	5α-androstan-3-one	12 ± 3	5.87
2α-hydroxyandrost-4-ene-3,17-dione	41 ± 6	5.16	4-androsten-16α-ol-3,17-dione	62 ± 2	4.79
1,4-androstadiene-3,17-dione	89 ± 2	4.09	5-pregnene-3,20-dione	45 ± 3	5.09
4-androstene-3,17-dione	56 ± 8	4.90	4-androsten-4-ol-3,17-dione	53 ± 3	4.95
androsterone	54 ± 8	4.93	dexamethasone	75 ± 11	4.52
5α-estran-3α-ol-17-one	91 ± 11	4.00	epitestosterone	73 ± 18	4.57
testosterone	78 ± 7	4.45	allo-pregnandione	73 ± 7	4.57
progesterone	53 ± 2	4.95	5α-androstan-17-one	45 ± 6	5.09
17α−hydroxyprogesterone	89 ± 1	4.09	1,(5α)-androstene-3,17-dione	90 ± 7	4.05
deoxycorticosterone	58 ± 2	4.86	5β-androstan-3α-ol	4 ± 1	6.38
cortexolone	88 ± 8	4.13	5α-androst-16-en-3β-ol	28 ± 6	5.41
5α-androstan-17β-ol-3-one	53 ± 6	4.95	dehydroepiandrosterone	71 ± 5	4.61
5α-androstane-3α,17b-diol	63 ± 3	4.77	4-androsten-6α-ol-3,17-dione	81 ± 14	4.37
5α-pregnan-3α-ol-20-one	19 ± 1	5.63	4-androsten-6β-ol-3,17-dione	89 ± 15	4.09
5α-androst-16-en-3-one	5 ± 1	6.28	5α-estrane-3,17-dione	80 ± 9	4.40
hydrocortisone	68 ± 6	4.67	estra-1,3,5(10)-trien-3-ol	56 ± 15	4.90
boldenon	69 ± 2	4.65	5α-androst-2-en-17-one	42 ± 4	5.14
corticosterone	80 ± 2	4.40	5α-pregnan-3-one	52 ± 8	4.97
5β-pregnane-3,20-dione	20 ± 7	5.60	4-androsten-3α-ol-17-one	66 ± 8	4.71
5α-androstan-3α-ol	4 ± 1	6.38			
4-androsten-11b-ol-3,17-dione	83 ± 9	4.31	4-androsten-7α-ol-3,17-dione*	97 ± 12	3.49
5α-androst-16-en-3α-ol	4 ± 1	6.38	pregnenolone*	95 ± 15	3.72

[a] The GAL4-mCAR LBD assays were performed as described in the Experimental section. The data are shown are normalized luciferase activity remaining at 10 μM steroid (expressed as percent of vehicle) and estimated pIC_{50} values (pIC_{50} = negative logarithm of IC_{50}). Vehicle control activity was 100 ± 9%. Asterisks (*) indicate outliers pregnenolone and 4-androsten-7α-ol-3,17-dione. All structures are available upon request from the authors.

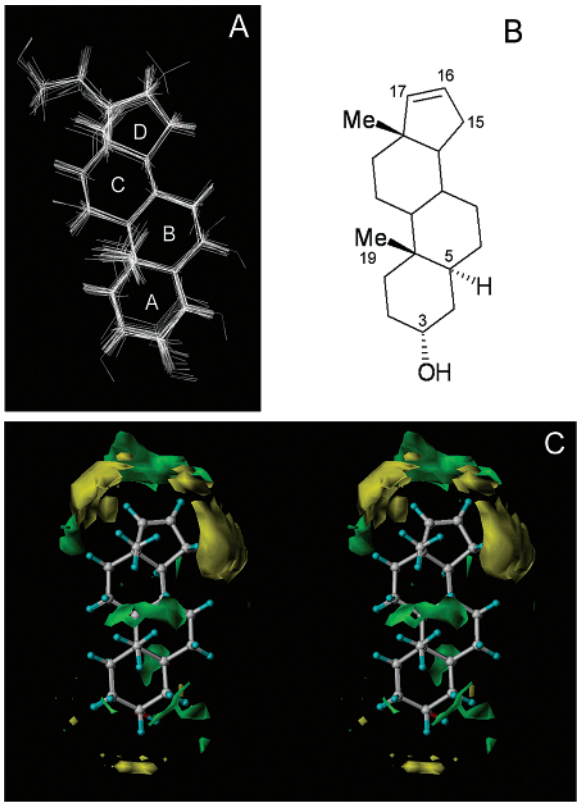

Figure 2. The molecular structures of the study compounds and the grid plot of the 3D-QSAR model. A. The energy-minimized structures of 43 steroids used for the GRID/GOLPE analysis were superimposed. The steroid rings A, B, C, and D are indicated. B. The two-dimensional structure of androstenol, with most important carbon atoms, is shown for reference. C. The PLS coefficient grid plot for water probe is shown. Coefficient levels −0.0005 are shown in yellow and 0.0005 in green in stereo image.

these features leads to weaker inhibition. Surroundings of the D-ring are quite restricting, since a large proportion of the nearby volume is disallowed. The only allowed area is in equatorial direction between positions C16 and C17. This allowed region is mostly explained by variation in the C17 substituents and to lesser extent by variation at C16. In contrast, axial substituents at C3 atom are more favorable than equatorial ones. In combination, these results suggest a restricted specificity of mCAR for inhibitors. According to this model, testosterone and progesterone, which possess C17β-hydroxyl and C17-acetyl substituents, respectively, a double bond at C4, and an equatorial substituent at C3, should both be modest inhibitors of mCAR. Indeed, this is exactly what is seen in cells: the respective IC_{50} values are about 35 and 11 μM (Table 1, Figure 1). This contrasts with results of Kawamoto et al., who reported a strong 70% and 90% inhibition by 10 μM testosterone and progesterone.[20]

Mechanisms of mCAR Inhibition. Mouse CAR activity, as measured above, is a net result from association of mCAR with a battery of corepressors and coactivators that are expressed in mammalian cells. Because both types of coregulators may, in principle, mediate the steroid-dependent inhibition, we compared the mCAR inhibition data to yeast two-hybrid assays with the well-established corepressor NCoR and coactivator SRC-1 as mCAR-interacting partners. The responses to TCPOBOP, three androstenol-like steroids, the "test set" compounds (ADIONE, ADIEN and AOCA), and reported mCAR inhibitors testosterone and progesterone were measured. The yeast two-hybrid system has been successfully used for studying interactions between various nuclear receptors and their coregulators in response to a large number of steroids, drugs, and xenobiotics.[15,22,24−28]

In mammalian cells, mCAR displayed substantial constitutive activity which was further activated by TCPOBOP (2.6-fold) and inhibited by 45−90% by androstenol-like steroids (Figure 3A). The "test set" compounds decreased basal mCAR activity by 25−67%. Testosterone and progesterone brought 20% and 50%

Table 2. Predicted and Experimental pIC50 Values of the "Test Set" Molecules[a]

molecule name	remaining activity at 10 μM (%)	experimental pIC_{50} value	predicted pIC_{50} value	difference between predicted and experimental pIC_{50}s
4-androstene-3-oxo-17β-carboxylic acid (AOCA)	81 ± 5	4.4	4.7	0.3
5α-androstane-3,17-dione (ADIONE)	34 ± 3	5.3	4.7	0.6
4,16-androstadien-3-one (ADIEN)	7 ± 2	6.1	5.9	0.2

[a] The predicted pIC_{50} values were calculated based on the created PLS model. The mCAR inhibition assays were performed as in Table 1.

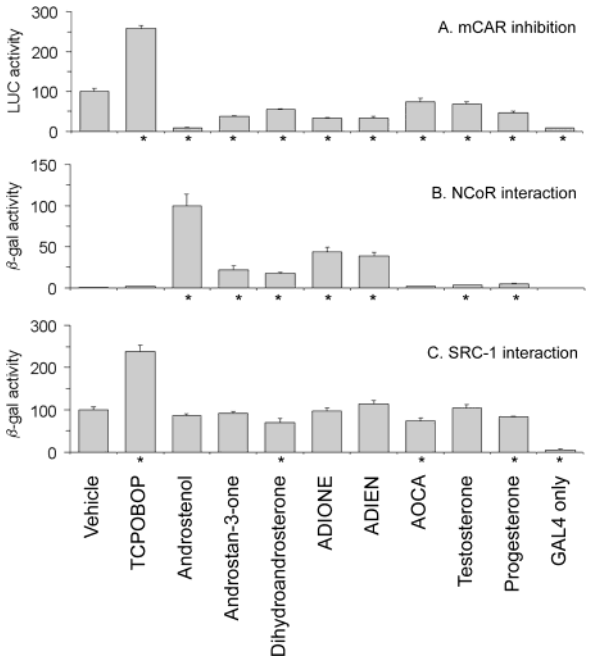

Figure 3. Comparison of mammalian inhibition data with yeast two-hybrid assays. A. Mouse CAR activity was measured after treatment with vehicle (set to 100), 1 μM TCPOBOP, and indicated 10 μM steroids. B, C. The same compounds were assayed for interaction between the mCAR LBD and the coregulators NCoR (B; androstenol set to 100) and SRC-1 (C; vehicle set to 100) in yeast. All assays contained a control that used the GAL4 only lacking the mCAR LBD. The data are means ± SD of at least three independent experiments. The asterisks below the columns indicate a statistically significant difference ($p < 0.05$) from the vehicle.

reduction in mCAR activity, respectively. When analyzed for ligand-induced association with corepressor NCoR (Figure 3B), TCPOBOP yielded no response while androstenol-like steroids enhanced the interaction between mCAR and NCoR. Of the "test set" compounds, potent inhibitors ADIONE and ADIEN strongly promoted mCAR−NCoR interaction (≈40% of androstenol response). The weaker inhibitors AOCA, testosterone, and progesterone exhibited much weaker NCoR association (≈5% or less of androstenol response, but significantly over vehicle control). These data indicated that there was a reasonably good correlation between the extents of mCAR inhibition and NCoR recruitment by the steroids ($r^2 = 0.79$, $n = 8$). The same compounds were used in the assay with the coactivator SRC-1 (Figure 3C). Similarly to data in Figure 3A, mCAR exhibited strong basal SRC-1 recruitment (compare vehicle vs GAL4 only) that was enhanced 2.4-fold by TCPOBOP. All steroids including the potent inhibitor androstenol had only modest effects on the mCAR−SRC-1 association (± 20%), which did not correlate at all with the extent of mCAR inhibition ($r^2 = 0.07$, $n = 8$). In summary, the inhibition of mCAR by steroids is mostly explained by their ability to induce interaction of mCAR with the corepressor NCoR. The weak inhibition caused by AOCA and progesterone may be due to slightly reduced interaction of mCAR with SRC-1.

Regions of mCAR Important for Androstenol Sensitivity. One noteworthy species difference between mCAR and hCAR is that the former is more sensitive to androstenol than the latter.[18,22] To search for regions important for androstenol sensitivity, we created various chimeric constructs between the mCAR and hCAR LBDs (Figure 4A). Figure 4B shows that mCAR was inhibited by more than 80% already at 1 μM androstenol while hCAR was inhibited only by 35% at 10 μM. Mouse/human chimeras showed that substitution of hCAR amino acids 108−190 with the corresponding mCAR residues 118−200 (*m1*) did not change the inhibition pattern of hCAR. Substitution of further 63 mCAR residues (*m2*) improved the sensitivity to inhibition so that already 1 μM androstenol produced a significant decrease in activity, close to a level observed with hCAR at 10 μM. Further substitution of 52 mCAR residues (*m3*) did not bring any additional improvement in inhibition. The reverse human/mouse chimeras showed that androstenol only inhibited the activity of the *h1* construct (that contained mCAR residues 201−358) but not of *h2* and *h3* chimeras. Thus, the region 201−263 in mCAR contributed significantly to androstenol sensitivity. In support of this, the double chimera *hmh* containing mCAR residues 201−263 on hCAR background was inhibited more than 50% by androstenol. In contrast, the inverse chimera *mhm* containing hCAR amino acids 191−253 on mCAR background was unresponsive. The mCAR lacking the helix 12 (*mΔ8*) was suppressed 50% by androstenol, while the GAL4 control (devoid of any LBD) did not react.

The same constructs were also tested for activation (Figure 4C). Human CAR was partially (40%) inhibited by EE2, not affected by TCPOBOP, and activated by clotrimazole while mCAR was activated by all three chemicals (Figure 4C), in line with our previous results.[22] The ability of EE2 (which is structurally reminiscent of androstenol) to increase reporter activity was retained by *m2* and *m3* but not by the *m1* chimera, while all these mouse/human chimeras were activated by clotrimazole, a common activator of both mCAR and hCAR. The observed increase in basal activity may explain the lower extent of activation with *m2* and *m3* constructs. Among the reverse chimeras, only the *h1* (but not *h2* or *h3*) construct responded to EE2. Even though the basal activities of these human/mouse chimeras were much reduced, they were still able to respond to clotrimazole so as to reach activities above the control (GAL4 only) level. This indicates that the chimeras were all functional. However, the attenuated

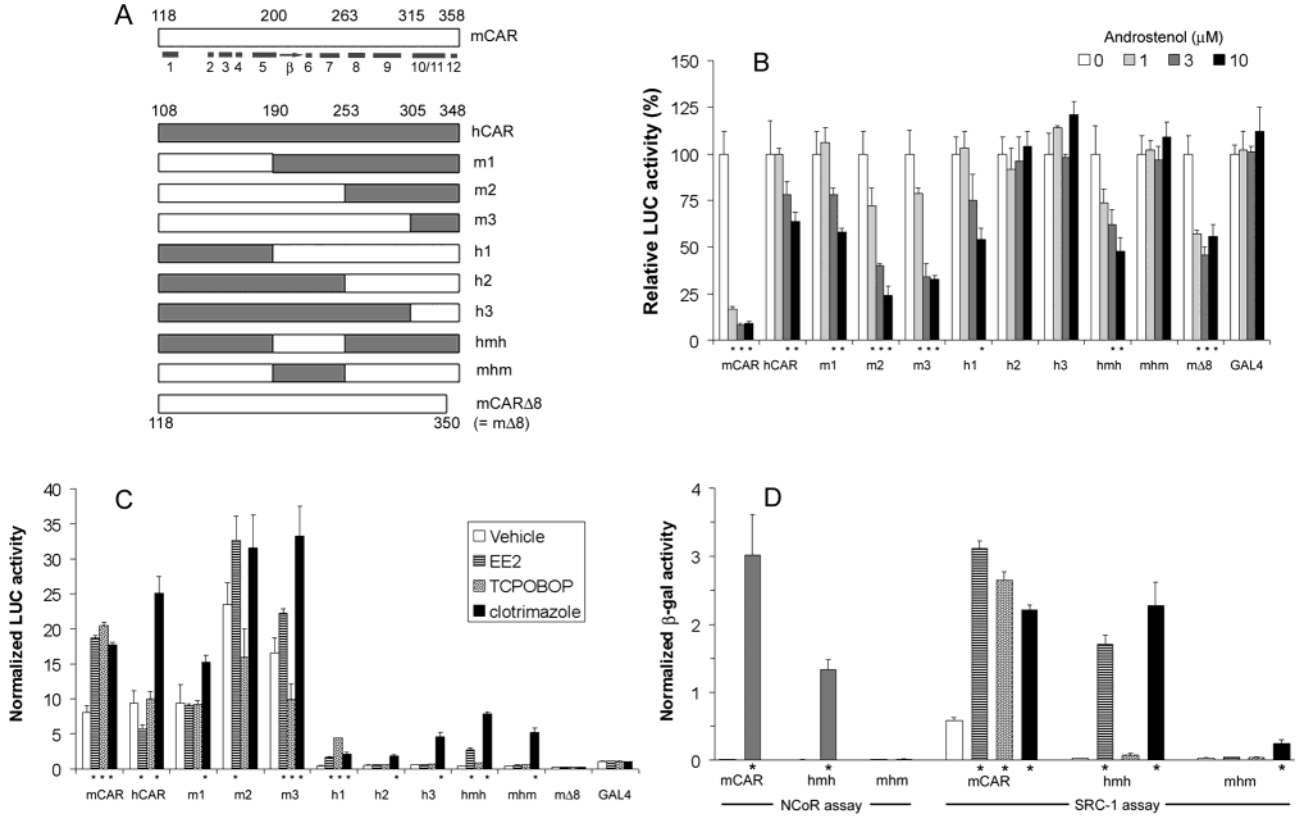

Figure 4. Analysis of CAR chimera. A. The LBD regions of mCAR (SwissProt # O35627; white), hCAR (SwissProt # Q14994; grey), and their indicated chimeras were constructed by DNA amplification. The N-terminus of mCAR, prior to the DBD, is 10 amino acids longer than that of hCAR. The junctions are indicated by corresponding mCAR/hCAR amino acid pairs (118/108, 200/190, 263/253, 315/305, and 358/348). The mCARΔ8 lacks eight C-terminal amino acids including helix 12. The predicted helices (1−12) and the β-sheet (β) are shown by boxes and an arrow, respectively. B. CAR activity was assayed as in Figure 1 after treatment with indicated concentrations of androstenol (0, 1, 3, 10 μM). The activity with vehicle (0 μM) was set to 100%. *C*. The basal and xenobiotic-induced activities of the same constructs were assayed after treatment with vehicle (□), 5 μM EE2 (crosshatched), 1 μM TCPOBOP (stippled), and 2 μM clotrimazole (■). The activity with GAL4 only with vehicle was set to unity. The data are means ± SD of four independent experiments. The asterisks below the columns indicate a statistically significant difference ($p < 0.05$) from the vehicle. D. The interaction of NCoR (left) and SRC-1 (right) with mCAR, hCAR, and their double chimeras *hmh* and *mhm* are shown after treatment with vehicle (□) and 10 μM androstenol (grey) (left panel) or with vehicle (□), 5 μM EE2 (crosshatched), 1 μM TCPOBOP (stippled), and 2 μM clotrimazole (■) (right panel). The data are means of normalized β-galactosidase activities ± SD of three independent experiments. The asterisks below the columns indicate a statistically significant difference ($p < 0.05$) from the vehicle.

basal activities of constructs *h1*, *hmh*, and *mΔ8* may explain why the extent of inhibition by androstenol (50−60%) could not reach the 90% level obtained with the more active wild-type mCAR. Finally, the double chimera *hmh* that was inhibited by androstenol also responded to EE2 while the inverse chimera *mhm* did not. The *mΔ8* construct did not react to any of the activators, as expected from the lack of helix 12. It is notable that *h1* (but not *hmh*) could respond to TCPOBOP, suggesting that residues C-terminal to 315 may contribute to recognition of this xenobiotic by mCAR. These results suggest that the region limited by mCAR amino acids 201 and 263 (helices 5−7) is important for sensitivity to androstenol inhibition and also to EE2 activation.

The above conclusion was supported by the yeast two-hybrid assays obtained with the double chimera *hmh* and *mhm* (Figure 4D). Only the former (*hmh*) responded to androstenol by recruiting NCoR while *mhm* did not. In the SRC-1 assay, both double chimeras displayed much reduced basal activity which was significantly increased by the common mCAR and hCAR activator clotrimazole. Only the *hmh* chimera responded to EE2 while both remained unresponsive to TCPOBOP. These results fully agree with the findings in Figures 4B and 4C and strongly indicate that the region 201−263 in mCAR is important for androstenol recognition and corepressor-mediated inhibition.

The importance of residues 201−263 appears to contrast with the recent report that residue 350 in helix 12 regulates the inhibition of mCAR by steroids.[29] Substitution of Thr350 with Met, the corresponding residue in hCAR, abolished the inhibition by progesterone and testosterone. However, the response to the potent inhibitor androstenol was not measured in that study.[29] Figure 5A indicates that mutation of Thr350 to Ala did not change the response of mCAR to steroids or TCPOBOP. Substitution of Thr350 with Met did not affect the inhibition by androstenol or testosterone. However, it specifically converted progesterone from an inhibitor to a ligand with an activating tendency. The response to TCPOBOP was decreased but not completely abolished with Thr350Met mutant. This finding is consistent with results from the *h1* and *hmh* chimeras (see Figure 4C) when the presence of hCAR residues in the C-terminus of the construct abrogated activation by

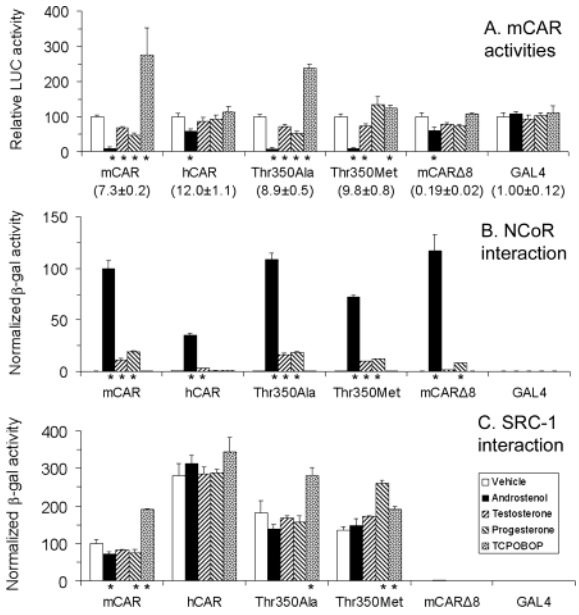

Figure 5. Analysis of helix 12 mutants. The indicated mCAR LBDs were assayed for response to vehicle (□), 10 μM androstenol (■), testosterone (hatched-up), progesterone (hatched-down), and TCPOBOP (stippled). In mammalian GAL4-mCAR LBD assay (A), the activity with vehicle was set to 100% for each receptor. Basal activities of these constructs, as compared to GAL4 (= 1.00), are shown in parentheses. In yeast assay with NCoR (B), activity with mCAR and androstenol was set to 100, and in yeast assay with SRC-1 (C) activity with mCAR and vehicle was set to 100. The data shown are means ± SD of at least three independent experiments. The asterisks below the columns indicate a statistically significant difference ($p < 0.05$) from the vehicle.

TCPOBOP. Steroids tended to decrease mCARΔ8-driven activity by 20−40% while GAL4 was unresponsive.

These findings were supported by yeast two-hybrid experiments. In corepressor assay (Figure 5B), interaction with NCoR was enhanced by androstenol and to lesser extent by progesterone and testosterone, regardless of the type of residue 350. Androstenol-elicited interaction of NCoR with hCAR was less efficient than with mCAR, as predicted by the weaker inhibition by androstenol of hCAR. Moreover, mCARΔ8 was able to recruit NCoR about as efficiently as the wild-type CAR in response to androstenol and progesterone. Figure 5C indicates that TCPOBOP enhanced SRC-1 interaction with mCAR and Thr350Ala mutant, to a lesser extent with Thr350Met mutant but not with hCAR. Deletion of helix 12 abolished both basal association with SRC-1 and any enhancement with TCPOBOP. Interestingly, SRC-1 interaction was enhanced by progesterone with Thr350Met mutant only, in agreement with data in Figure 5A. In summary, these data show that the general steroid-dependent inhibition of mCAR and its association with corepressors does not depend on the type of residue 350.

Discussion

Assay and Modeling of mCAR Inhibitors. There is increasing interest in predicting binding of chemicals to NRs such as pregnane X receptor and CAR that regulate genes involved in drug and steroid metabolism. Although protein homology modeling may be a reasonable tool for screening in silico, it should be complemented with reliable experimental data, especially when ligand binding can lead to very opposing effects as is the case with CAR. In fact, it is not clear from current models of ligand docking how inverse agonists of CAR[30] or antagonists of pregnane X receptor[31] mediate their suppressive effects and which structural properties of these ligands are important for such suppression.

To better understand the steroid-mediated inhibition of mCAR, we devised a GAL4-mCAR LBD-based assay that seems to meet several criteria required in QSAR development. First, the pattern of inhibition by various steroids and their IC_{50} values match very well with those obtained with the full-length mCAR system and agree with previous reports on inhibition by androstenol ($IC_{50} \approx 0.25-0.4$ μM) and testosterone ($IC_{50} > 10$ μM).[15,17] Second, the assay is based on a single effector site (mCAR LBD) and not dependent on factors such as mCAR-DNA interactions, heterodimerization with RXR, or chromatin packing. According to present experiments, the first two factors do not seem to have a major impact on steroid inhibition. Chromatin packing is also unlikely to be important because a cell line carrying genomic copies of both full-length mCAR and the PBREM-tk-luc reporter could be suppressed with similar potency by androstenol ($IC_{50} \approx 0.3$ μM).[19] It should be noted here that most known NR inhibitors act through binding to the LBD.[1]

The mCAR LBD appears rather selective for inhibitors. Out of 43 steroids tested, only 3-hydroxy and 3-keto steroids that had no substituents or an acetyl group attached to C17 proved to be effective inhibitors ($IC_{50} < 10$ μM). Addition of a double bond in the A-ring, a hydroxyl group at C17 in the D-ring, or removal of the C19 methyl group caused an increase in IC_{50}. The ability to predict novel mCAR inhibitors well indicates the reliability of the present QSAR model: pIC_{50} values could be predicted within 0.3 log units for two unknown steroids, and all three were predicted to an accuracy of 0.6 log units or better. A recent report on aryl sulfotransferase, which utilized similar methods for modeling but included protein structural information, could predict six substrates to a similar accuracy of 0.24−1.04 log units.[32] The good prediction power of the current model implies that the mCAR androstenol binding site is highly restrictive.

Mechanisms of mCAR Inhibition. There was a strong correlation between the mCAR inhibition potential and the ability to induce mCAR−NCoR interaction with different steroids. In contrast, all steroids including androstenol displayed very modest suppression of mCAR−SRC-1 interaction that did not reflect the extent of mCAR inhibition. Also, the removal of helix 12 did not abolish interaction of mCAR with androstenol or other inhibitory steroids. These data strongly suggest that the main mechanism of mCAR inhibition by steroids in general is via recruitment of corepressors. In support of this idea, androstanol was recently shown to enhance interactions of the corepressor SMRT between mCAR with a mammalian two-hybrid assay in CV-1 cells.[33]

Ueda et al. reported that testosterone and progesterone inhibited mCAR depending on type of residue 350, and thus this residue would directly regulate steroid-responsiveness of mCAR.[29] They also showed that

overexpression of SRC-1 prevented the suppression by progesterone of wild-type mCAR but not Thr350Met mutant, which implied that progesterone might inhibit mCAR through dissociation of SRC-1. Our data indicated only a slight decrease by progesterone in association between mCAR and SRC-1, which is consistent with the preceding view. It should be pointed out that, in comparison with androstenol-like potent inhibitors, progesterone is a weaker inhibitor and also quite ineffective in recruiting NCoR to mCAR. Our data also indicate that the role of residue 350 in steroid inhibition is limited: the Thr350Ala mutant behaved exactly like the wild-type mCAR, and the responses to androstenol or testosterone are not changed by either Ala or Met mutations. The striking difference was that conversion of Thr350 to Met changed progesterone to an activator in both mammalian and yeast assays. This implies that progesterone is able to bind to the mCAR ligand-binding pocket, perhaps in multiple orientations. These distinct orientations may explain why progesterone enhanced interactions of the Thr350Met mutant with both NCoR and SRC-1. Moreover, mCAR lacking the entire helix 12 was still able to recruit NCoR in response to androstenol and also testosterone and progesterone, suggesting that amino acids in helix 12 including Thr350 are not essential for steroid recognition. Other amino acids such as Lys187 and Phe171 *plus* Ile174 have been shown to affect corepressor binding[33] and responsiveness to both TCPOBOP and androstenol,[17] respectively. However, because Lys187 is conserved among NRs and it forms a crucial contact with both coactivators and corepressors,[4,5] and because the double mutation of Phe171 *plus* Ile174 to alanine abolished the response to both activating and inhibiting ligands,[17] we interpret that these amino acids have a more global role in mCAR function. Thus, they would not be directly linked to specific steroid recognition by mCAR, which was the focus of this investigation and the suggested role for the residue Thr350.[29]

On the basis of a homology model built on the pregnane X receptor, it was hypothesized that androstenol might bind to the mCAR coactivator surface (and not to the ligand-binding pocket) due to its mimicry of hydrophobic residues Leu352, Leu353, Ile356, and Cys357 in helix 12. The resulting competition by androstenol with helix 12 for binding to this surface would thus explain the inhibitory activity.[33] Our data cannot exclude this hypothesis, although it is difficult to reconcile with other findings. First, there are wide differences in inhibition of mCAR by structurally very similar steroids that could be expected to equally mimic the hydrophobic residues in helix 12. Second, mCAR and hCAR are differentially sensitive to androstenol, yet they possess identical 'androstenol-mimicking' residues in helix 12 and a high degree of similar residues (10/13) within the putative androstenol-binding pocket.[33] The NR surface for coactivator and corepressor binding,[34,35] which shares amino acids with the putative pocket, is covered by mCAR residues 176−209. This stretch overlaps the helices 5−7 by only nine residues (201−209), which are identical between mCAR and hCAR receptors and thus cannot explain the receptors' differential sensitivity toward androstenol. An alternative explanation is that androstenol binds to the mCAR ligand-binding pocket. This view is supported by the observed importance of helices 5−7 which form a critical part of the ligand-binding pocket in closely related vitamin D and pregnane X receptors.[36,37] Only three out of 10 residues lining the putative androstenol-binding pocket are contained within helices 5−7,[33] and these three (Lys205, Ala208, and Val209) are identical in mCAR and hCAR. We have not yet been able to pinpoint the exact amino acid(s) critical for androstenol response. This suggests that several residues contribute to the binding specificity.

Conclusions

We have developed a 3D-QSAR model for mCAR inhibitors that could well predict the response by unknown steroids, and two novel inhibitors were identified. The mechanism of steroid-elicited mCAR inhibition proceeds mainly by steroid-dependent recruitment of corepressors, with only minor contribution from dissociation of coactivators. A central region in mCAR LBD is required for androstenol inhibition while the residue 350 in helix 12 does not seem to play a general role in steroid recognition, as proposed previously. Our results clarify the ligand specificity and mechanisms of action of mCAR.

Experimental Section

Chemicals. Steroids were purchased from Steraloids Inc. (Newport, RI). Other chemicals were at least analytical grade from Sigma (St. Louis, MO). The synthesis and verification of TCPOBOP has been described.[22] Deoxyoligonucleotides were bought from Sigma-Genosys (Cambridge, UK).

Plasmids. PBREM-tk-luc reporter with the natural *Cyp2b10* response element, full-length mCAR and human CAR (hCAR) expression plasmids, and GAL4 fusions of mCAR and hCAR LBDs have been described.[19,22] CMX-GAL4 expression vector and GAL4-responsive UASx4-tk-luc reporter were kind gifts from Prof. R. M. Evans (Salk Institute, La Jolla, CA). Transfection control plasmid pCMVβ was purchased from Clontech, Inc. (Palo Alto, CA). Mouse CARΔ8 lacking helix 12,[14] and various chimera between mCAR and hCAR, were generated by standard DNA amplification protocols.[38] Point mutations into the mCAR LBD were done according to QuikChange mutagenesis kit (Stratagene, La Jolla, CA). Every chimeric or mutant LBD generated by DNA amplification was sequenced over the amplified region. All plasmids were purified with Qiagen columns (Hilden, Germany).

Mammalian mCAR Inhibition Assays. HEK293 cells were cultured in 48-well plates as described.[22] Cells at 50% confluence were transfected with pCMVβ (25 ng), full-length mCAR or GAL4-LBD construct (6.25 ng), and PBREM-tk-luc or UASx4-tk-luc reporter construct (12.5 ng), respectively, per well by the calcium phosphate method for 4 h. The cells were then washed with PBS, and fresh medium supplemented with 5% delipidated serum containing either vehicle or test chemical (up to 30 μM) was added. The mCAR agonist TCPOBOP (1 μM) and inverse agonist androstenol (10 μM) were used as positive and negative controls, respectively. Cells were cultured for 40 h post-transfection, washed with PBS, and lysed. Luciferase and β-galactosidase activities were determined from 20 μL of lysates in 96-well plates using the Victor2 multiplate reader (PerkinElmer Wallac, Turku, Finland).[19] All luciferase activities were normalized to β-galactosidase expression and expressed as means ± standard deviation from three or four independent experiments. When appropriate, Student's *t*-test was used to compare activities between vehicle and chemical treatments.

Molecular Modeling. In this study, 3D-QSAR is used to quantitatively explain structure−activity relationships of

mCAR inhibitors, allowing the visualization of biologically important structural properties. All molecular modeling and QSAR studies were performed on an SGI Octane2 workstation. The structures of the steroids used are available upon request from the authors. Construction of the molecules and superimposition was done with Sybyl 6.8 (Tripos Inc., St. Louis, MO). The molecular structures were searched from Cambridge Structural Database,[39] or if not present there, created using the sketch option in Sybyl, and structures were further minimized with the MMFF94 force field.[40] Minimized molecules were superimposed as shown in Figure 2A by using a rigid fit. The 3D-QSAR analysis was made using GOLPE 4.5 (Multivariate Informetric Analysis, Perugia, Italy) and GRID version 20 (Molecular Discovery Limited, Oxford, England) with the default water probe.[41,42] The GOLPE/GRID method correlates molecular interaction fields with the biological activity using a multivariate partial least squares (PLS) method. Here, water probe−steroid interactions fields are correlated with steroid-elicited mCAR inhibition. The mCAR inhibition data were derived with first screening at 1 and 10 μM concentration. Then, we used 4−7 doses in the range of 0.01 to 30 μM in case of notable inhibitors (more than 20% inhibition) or with 2−3 doses with less efficient inhibitors. The inhibition data were transformed to pIC_{50} values using the logit transformation (pIC_{50} = negative logarithm of IC_{50}). The grid spacing was 0.5 Å, and the standard deviation threshold for exclusion of data columns from the PLS analysis was set at 0.1 kcal/mol. All two- and three-level variables were removed, and values between −0.01 and 0.1 were zeroed. Smart region definition (SRD)[43] with F-factorial selection was used with two PLS-components in the selection and validation phase, together with 10 random group PLS validations. The optimum number of PLS components was selected by using a cross-validation with five groups to derive the lowest standard error of prediction (SDEP); this calculation was repeated 20 times. The number of PLS components was not allowed to be higher than five to ensure simplicity of the model. From cross-validation predictions, a q^2-value is derived. Typically, q^2-values above 0.5 indicate an internally consistent and valid model.[23] The external SDEP was calculated by predicting the inhibition activity of three compounds not belonging to the original data set, namely 4-androstene-3-oxo-17β-carboxylic acid (AOCA), 5α-androstane-3,17-dione (ADIONE), and 4,16-androstadien-3-one (ADIEN) (later referred to as the "test set").

Yeast Two-Hybrid Assays. Plasmids in the Matchmaker GAL4 System 3 (Clontech) were used. Various LBDs were inserted into pGBKT7 plasmid, and the NR interaction domain (residues 1988−2304) from mouse corepressor NCoR[44] was cloned from liver RNA and inserted into pGADT7 plasmid as described.[22] The NR interaction domain (residues 549−789) from mouse SRC-1[45] was amplified similarly and inserted between *Nde*I and *Bam*HI sites of pGADT7 plasmid. All manipulations were done according to manufacturer's instructions. Yeast colonies that expressed both CAR LBD and the interacting partner (NCoR or SRC-1) were selected on SD plates lacking both leucine and tryptophan. Randomly picked colonies were amplified, and aliquots of yeast cells were treated with vehicle or steroids for 3.5 h before measurement of cell density, β-galactosidase activity, and turbidity. [22,24]

Appendix

Abbreviations used: ADIEN, 4,16-androstadien-3-one; ADIONE, 5α-androstane-3,17-dione; AOCA, 4-androstene-3-oxo-17β-carboxylic acid; CAR, constitutive androstane receptor; CYP, cytochrome P450; DBD, DNA-binding domain; EE2, 17α-ethynyl-3,17β-estradiol; LBD, ligand-binding domain; NCoR, nuclear receptor corepressor; NR, nuclear receptor; PB, phenobarbital; PBREM, PB-responsive enhancer module; PLS, partial least squares; QSAR, quantitative structure−activity relationship; RXR, retinoid X receptor; SDEP, standard error of prediction; SRC-1, steroid receptor coactivator-1; SRD, smart region definition; TCPOBOP, 1,4-bis[2-(3,5-dichloropyridyloxy)]benzene.

Acknowledgment. We thank Prof. Ronald Evans for plasmids, and Ms. Kaarina Pitkänen for technical assistance. This study was supported by the Academy of Finland (grants 44040 and 51610 to P.H.).

References

(1) Weatherman, R. V.; Fletterick, R. J.; Scanlan, T. S. Nuclear Receptor Ligands and Ligand-Binding Domains. *Annu. Rev. Biochem*. **1999**, *68*, 559−581.
(2) Chawla, A.; Repa, J. J.; Evans, R. M.; Mangelsdorf, D. J. Nuclear Receptors and Lipid Physiology: Opening the X-Files. *Science* **2001**, *294*, 1866−1870.
(3) Maglich, J. M.; Sluder, A.; Guan, X.; Shi, Y.; McKee, D. D.; Carrick, K.; Kamdar, K.; Willson, T. M.; Moore, J. T. Comparison of Complete Nuclear Receptor Sets from the Human, *Caenorhabditis elegans* and *Drosophila* Genomes. *Genome Biol*. **2001**, *2*, RESEARCH0029.
(4) Moras, D.; Gronemeyer, H. The Nuclear Receptor Ligand-Binding Domain: Structure and Function. *Curr. Opin. Cell. Biol*. **1998**, *10*, 384−391.
(5) Bourguet, W.; Germain, P.; Gronemeyer, H. Nuclear Receptor Ligand-Binding Domains: Three-Dimensional Structures, Molecular Interactions and Pharmacological Implications. *Trends Pharmacol. Sci*. **2000**, *21*, 381−388.
(6) Rosenfeld, M. G.; Glass, C. K. Coregulator Codes of Transcriptional Regulation by Nuclear Receptors. *J. Biol. Chem*. **2001**, *276*, 36865−36868.
(7) Hu, X.; Lazar, M. A. Transcriptional Repression by Nuclear Hormone Receptors. *Trends Endocrinol. Metab*. **2000**, *11*, 6−10.
(8) Pike, A. C.; Brzozowski, A. M.; Hubbard, R. E.; Bonn, T.; Thorsell, A. G.; Engström, O.; Ljunggren, J.; Gustafsson J.-Å.; Carlquist, M. Structure of the Ligand-Binding Domain of Oestrogen Receptor Beta in the Presence of a Partial Agonist and a Full Antagonist. *EMBO J*. **1999**, *18*, 4608−4618.
(9) Honkakoski, P.; Zelko, I.; Sueyoshi, T.; Negishi, M. The Orphan Nuclear Receptor CAR−Retinoid X Receptor Heterodimer Activates the Phenobarbital-Responsive Enhancer Module of the *CYP2B* Gene. *Mol. Cell. Biol*. **1998**, *18*, 5652−5658.
(10) Wei, P.; Zhang, J.; Egan-Hafley, M.; Liang, S.; Moore, D. D. The Nuclear Receptor CAR Mediates Specific Xenobiotic Induction of Drug Metabolism. *Nature* **2000**, *407*, 920−923.
(11) Honkakoski, P.; Negishi, M. Regulation of Cytochrome P450 (*CYP*) Genes by Nuclear Receptors. *Biochem. J*. **2000**, *347*, 321−337.
(12) Willson, T. M.; Kliewer, S. A. PXR, CAR and Drug Metabolism. *Nat. Rev. Drug Discovery* **2002**, *1*, 259−266.
(13) Ueda, A.; Hamadeh, H. K.; Webb, H. K.; Yamamoto, Y.; Sueyoshi, T.; Afshari, C. A.; Lehmann, J. M.; Negishi, M. Diverse Roles of the Nuclear Orphan Receptor CAR in Regulating Hepatic Genes in Response to Phenobarbital. *Mol. Pharmacol*. **2002**, *61*, 1−6.
(14) Choi, H. S.; Chung, M.; Tzameli, I.; Simha, D.; Lee, Y. K.; Seol, W.; Moore, D. D. Differential *Trans*-Activation by Two Isoforms of the Orphan Nuclear Hormone Receptor CAR. *J. Biol. Chem*. **1997**, *272*, 23565−23571.
(15) Forman, B. M.; Tzameli, I.; Choi, H. S.; Chen, J.; Simha, D.; Seol, W.; Evans, R. M.; Moore, D. D. Androstane Metabolites Bind to and Deactivate the Nuclear Receptor CAR-β. *Nature* **1998**, *395*, 612−615.
(16) Sueyoshi, T.; Kawamoto, T.; Zelko, I.; Honkakoski, P.; Negishi, M. The Repressed Nuclear Receptor CAR Responds to Phenobarbital in Activating the Human *CYP2B6* Gene. *J. Biol. Chem*. **1999**, *274*, 6043−6046.
(17) Tzameli, I.; Pissios, P.; Schuetz, E. G.; Moore, D. D. The Xenobiotic Compound 1,4-Bis[2-(3,5-Dichloropyridyloxy)]Benzene Is an Agonist Ligand for the Nuclear Receptor CAR. *Mol. Cell. Biol*. **2000**, *20*, 2951−2958.
(18) Moore, L. B.; Parks, D. J.; Jones, S. A.; Bledsoe, R. K.; Consler, T. G.; Stimmel, J.; Goodwin, B.; Liddle, C.; Blanchard, S. G.; Willson, T. M.; Collins, J. L.; Kliewer, S. A. Orphan Nuclear Receptors Constitutive Androstane Receptor and Pregnane X Receptor Share Xenobiotic and Steroid Ligands. *J. Biol. Chem*. **2000**, *275*, 15122−15127.
(19) Honkakoski, P.; Jääskelainen, I.; Kortelahti, M.; Urtti, A. A Novel Drug-Regulated Gene Expression System Based on the Nuclear Receptor Constitutive Androstane Receptor (CAR). *Pharm. Res*. **2001**, *18*, 146−150.

(20) Kawamoto, T.; Kakizaki, S.; Yoshinari, K.; Negishi, M. Estrogen Activation of the Nuclear Orphan Receptor CAR (Constitutive Active Receptor) in Induction of the Mouse *Cyp2b10* Gene. *Mol. Endocrinol.* **2000**, *14*, 1897−1905.
(21) Min, G.; Kemper, J. K.; Kemper, B. Glucocorticoid Receptor-Interacting Protein 1 Mediates Ligand-Independent Nuclear Translocation and Activation of Constitutive Androstane Receptor In Vivo. *J. Biol. Chem.* **2002**, *277*, 26356−26363.
(22) Mäkinen, J.; Frank, C.; Jyrkkärinne, J.; Gynther, J.; Carlberg, C.; Honkakoski, P. Modulation of Mouse and Human Phenobarbital-Responsive Enhancer Module by Nuclear Receptors. *Mol. Pharmacol.* **2002**, *62*, 366−378.
(23) Clark, M.; Cramer, R. D. The Probability of Chance Correlation Using Partial Least Squares. *Quant. Struct.-Act. Relat.* **1993**, *12*, 137−145.
(24) Nishikawa, J.; Saito, K.; Goto, J.; Dakeyama, F.; Matsuo, M.; Nishihara, T. New Screening Methods for Chemicals with Hormonal Activities Using Interaction of Nuclear Hormone Receptor with Coactivator. *Toxicol. Appl. Pharmacol.* **1999**, *154*, 76−83.
(25) Masuayama, H.; Hiramatsu, Y.; Kunitomi, M.; Kudo, T.; MacDonald, P. N. Endocrine Disrupting Chemicals Phthalic Acid and Nonylphenol Activate Pregnane X Receptor-Mediated Transcription. *Mol. Endocrinol.* **2000**, *14*, 421−428.
(26) Nishihara, T.; Nishikawa, J.; Kanayama, T.; Dakeyama, F.; Saito, K.; Imagawa, M.; Takatori, S.; Kitagawa, Y.; Hori, S.; Utsumi, H. Estrogenic Activities of 517 Chemicals by Yeast Two-Hybrid Assay. *J. Health Sci.* **2000**, *46*, 282−298.
(27) Nagpal, S.; Ghosn, C. R.; Chandraratna, R. A. S. Identification of Nuclear Receptor Interacting Proteins Using Yeast Two-Hybrid Technology. *Methods Mol. Biol.* **2001**, *176*, 359−376.
(28) Lee, H.-S.; Miyauchi, K.; Nagata, Y.; Fukuda, R.; Sasagawa, S.; Endoh, H.; Kato, S.; Horiuchi, H.; Takagi, M.; Ohta, A. Employment of the Human Estrogen Receptor β Ligand-Binding Domain and Co−Activator SRC1 Nuclear Receptor-Binding Domain for the Construction of a Yeast Two-Hybrid Detection System for Endocrine Disrupters. *J. Biochem.* **2002**, *131*, 399−405.
(29) Ueda, A.; Kakizaki, S.; Negishi, M.; Sueyoshi, T. Residue Threonine 350 Confers Steroid Hormone Responsiveness to the Mouse Nuclear Orphan Receptor CAR. *Mol. Pharmacol.* **2002**, *61*, 1284−1288.
(30) Xiao, L.; Cui, X.; Madison, V.; White, R. E.; Cheng, K.-C. Insights from a Three-Dimensional Model into Ligand Binding to Constitutive Active Receptor. *Drug Metab. Dispos.* **2002**, *30*, 951−956.
(31) Ekins, S.; Erickson, J. A. A Pharmacophore for Human Pregnane X Receptor. *Drug Metab. Dispos.* **2002**, *30*, 96−99.
(32) Sharma, V.; Duffel, M. W. Comparative Molecular Field Analysis of Substrates for an Aryl Sulfotransferase Based on Catalytic Mechanism and Protein Homology Modeling. *J. Med. Chem.* **2002**, *45*, 5514−5522.
(33) Dussault, I.; Lin, M.; Hollister, K.; Fan, M.; Termini, J.; Sherman, M. A.; Forman, B. M. A Structural Model of the Constitutive Androstane Receptor Defines Novel Interactions That Mediate Ligand-Independent Activity. *Mol. Cell. Biol.* **2002**, *22*, 5270−5280.
(34) Steinmetz, A. C. U.; Renaud, J.-P.; Moras, D. Binding of Ligands and Activation of Transscription by Nuclear Receptors. *Annu. Rev. Biophys. Biomol. Struct.* **2001**, *30*, 329−359.
(35) Xu, E. X.; Stanley, T. B.; Montana, V. G.; Lambert, M. H.; Shearer, B. G.; Cobb, J. E.; McKee, D. D.; Galardi, C. M.; Plunket, K. D.; Nolte, R. T.; Parks, D. J.; Moore, J. T.; Kliewer, S. A.; Willson, T. M.; Stimmel, J. B. Structural Basis for Antagonist-Mediated Recruitment of Nuclear Co−Repressors by PPARα. *Nature* **2002**, *415*, 813−817.
(36) Rochel, N.; Wurtz, J. M.; Mitschler, A.; Klaholz, B.; Moras, D. The Crystal Structure of the Nuclear Receptor for Vitamin D Bound to Its Natural Ligand. *Mol. Cell* **2000**, *5*, 173−179.
(37) Watkins, R. E.; Wisely, G. B.; Moore, L. B.; Collins, J. L.; Lambert, M. H.; Williams, S. P.; Willson T. M.; Kliewer S. A.; Redinbo, M. R. The Human Nuclear Xenobiotic Receptor PXR: Structural Determinants of Directed Promiscuity. *Science* **2001**, *292*, 2329−2333.
(38) Sambrook, J.; Russell, D. W. *Molecular Cloning*, 3rd ed.; CSHL Press: New York, 2001.
(39) Allen, F. H.; Kennard, O. 3D Search and Research Using the Cambridge Structural Database. *Chem. Design Automat. News* **1993**, *8*, 31−37.
(40) Halgren, T. A. Merck Molecular Force field. I. Basis, Form, Scope, Parametrization, and Performance of MMFF94. *J. Comput. Chem.* **1996**, *17*, 490−519.
(41) Baroni, M.; Costantino, G.; Cruciani, G.; Riganelli, D.; Valigi, R.; Clementi, S. Generating Optimal Linear PLS Estimates (GOLPE): An Advanced Chemometric Tool for Handling 3D-QSAR Problems. *Quant. Struct.-Act. Relat.* **1993**, *12*, 9−20.
(42) Goodford, P. J. A Computational Procedure for Determining Energetically Favorable Binding Sites on Biologically Important Macromolecules. *J. Med. Chem.* **1985**, *28*, 849−857.
(43) Pastor, M.; Cruciani, G.; Clementi, S. Smart Region Definition: A New Way to Improve the Predictive Ability and Interpretability of Three-Dimensional Quantitative Structure−Activity Relationships. *J. Med. Chem.* **1997**, *40*, 1455−1464.
(44) Hu, X.; Lazar, M. A. The CoRNR Motif Controls the Recruitment of Corepressors by Nuclear Hormone Receptors. *Nature* **1999**, *402*, 93−96.
(45) Oñate, S. A.; Tsai, S. Y.; Tsai, M. J.; O'Malley, B. W. Sequence and Characterization of a Coactivator for the Steroid Hormone Receptor Superfamily. *Science* **1995**, *270*, 1354−1357.

JM030861T